Modulation of dynamic modes by interplay between positive and negative feedback loops in gene regulatory networks

Liu-Suo Wang,[1,2] Ning-Xi Li,[2] Jing-Jia Chen,[1] Xiao-Peng Zhang,[1,2,*] Feng Liu,[2,†] and Wei Wang[2]

[1]*Kuang Yaming Honors School, Nanjing University, Nanjing 210023, China*

[2]*National Laboratory of Solid State Microstructures, Department of Physics, and Collaborative Innovation Center of Advanced Microstructures, Nanjing University, Nanjing 210093, China*

(Received 4 June 2017; revised manuscript received 25 January 2018; published 16 April 2018; corrected 8 January 2020)

A positive and a negative feedback loop can induce bistability and oscillation, respectively, in biological networks. Nevertheless, they are frequently interlinked to perform more elaborate functions in many gene regulatory networks. Coupled positive and negative feedback loops may exhibit either oscillation or bistability depending on the intensity of the stimulus in some particular networks. It is less understood how the transition between the two dynamic modes is modulated by the positive and negative feedback loops. We developed an abstract model of such systems, largely based on the core p53 pathway, to explore the mechanism for the transformation of dynamic behaviors. Our results show that enhancing the positive feedback may promote or suppress oscillations depending on the strength of both feedback loops. We found that the system oscillates with low amplitudes in response to a moderate stimulus and switches to the on state upon a strong stimulus. When the positive feedback is activated much later than the negative one in response to a strong stimulus, the system exhibits long-term oscillations before switching to the on state. We explain this intriguing phenomenon using quasistatic approximation. Moreover, early switching to the on state may occur when the system starts from a steady state in the absence of stimuli. The interplay between the positive and negative feedback plays a key role in the transitions between oscillation and bistability. Of note, our conclusions should be applicable only to some specific gene regulatory networks, especially the p53 network, in which both oscillation and bistability exist in response to a certain type of stimulus. Our work also underscores the significance of transient dynamics in determining cellular outcome.

DOI: 10.1103/PhysRevE.97.042412

I. INTRODUCTION

Positive and negative feedback loops act as key regulatory elements in gene regulatory networks. A negative feedback loop (NFL) alone can induce oscillations or cellular homeostasis [1], while a positive feedback loop (PFL) can evoke bistability, which may underlie cell fate decision [2]. Nevertheless, feedback loops are usually interlinked rather than working separately to perform various functions [3]. It is still a challenge to uncover the emergent functions resulting from interlinked feedback loops.

Design principles underlying coupled feedback loops have attracted extensive attention in computational systems biology. It has been revealed that linking fast and slow PFLs produces a sensitive switch with strong robustness in cell signaling [3–5]. Recently, more efforts have been made to explore the performance advantages of interlinked positive and negative feedback loops (IPNFLs) from different aspects [6–9]. Pomerening *et al.* reported that the PFL and NFL cooperate to create a relaxation oscillator in which the PFL is essential for sustained oscillations [6]. Tsai *et al.* further proposed that IPNFLs allow for tunable and robust oscillations with widely tunable frequency and nearly constant amplitude [7]. From a distinct perspective, we found that IPNFLs exhibit bistability, excitability, or oscillation when the strength of feedback loops is changed [9]. These studies mostly focused on the steady-state properties rather than the transient dynamics of IPNFLs. It is worthwhile to explore the transient dynamics and their functional implications in the cellular stress response.

IPNFLs can produce rich dynamics depending on the network topology, relative strength of feedback, and intensity of stimuli. We aim at some particular gene regulatory networks in which IPNFLs can induce either oscillation or switchlike behavior in the same cellular response. In the DNA damage response, for example, p53-induced Mdm2 and PTEN feedback to inhibit and activate p53, respectively, enclosing an NFL and a PFL [10] [Fig. 1(a)]. It was reported that p53 shows bimodal dynamics depending on the strength of DNA damage, i.e., the p53 level undergoes periodic pulses upon mild damage or rises monotonically after extremely severe damage [11]. It was recently observed that p53 oscillates in the early phase and switches to a high level in the late phase in response to severe damage [12], referred to as two-phase dynamics in our modeling work [13]. In response to hypoxia, HIF-1 induces PHD2, which promotes its degradation to enclose an NFL [14]. HIF-1 also induces microRNAs like miR-182 to inhibit PHD2 production, forming a PFL [15,16] [Fig. 1(b)]. Consequently, HIF-1 shows oscillations alone or sustained

*zhangxp@nju.edu.cn

†fliu@nju.edu.cn

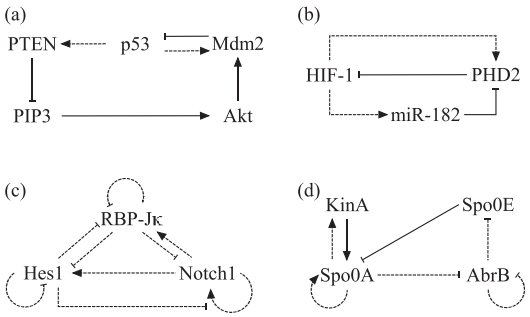

FIG. 1. Examples of biological systems with interlinked positive and negative feedback loops. (a) p53-centered feedback loops involved in the DNA damage response. (b) The HIF-1 system in response to hypoxia. (c) Positive and negative feedback loops in the Notch1-Hes1 crosstalk network. (d) Feedback loops modulating the competition between sporulation and competence in *Bacillus subtilis*. The transactivation and transrepression of genes are represented by arrow- and bar-headed dashed lines, respectively. The activation and inhibition of the proteins are separately denoted by arrow- and bar-headed solid lines.

high levels following oscillations [17]. Responsible for cell development, Notch1 and its downstream transcription factors Hes1 and RBP-Jκ constitute an intricate network of PFL and NFL [18,19] [Fig. 1(c)]. It has been reported that Hes1 exhibits oscillations or sustained activation, leading to different cellular outcomes in stem cell differentiation [20,21]. In the competence or sporulation decision process in *Bacillus subtilis*, the Spo0A-AbrB-Spo0E NFL and Spo0A-KinA PFL interlink to control the initiation of sporulation. The NFL first induces pulses of Spo0A, while the delayed PFL progressively ratchets up the amplitude of Spo0A pulsing until the amplitude exceeds some threshold to initiate sporulation [22–24] [Fig. 1(d)]. In the above examples, IPNFLs produce switchlike dynamics after transient oscillations in response to a certain type of stimulus. It is intriguing to explore the common mechanism underlying the transition between different dynamic modes in these gene regulatory networks.

To be specific, we focused on the core p53 regulatory network and developed an abstract model of IPNFLs to illuminate the mechanism of the transition between different dynamic modes. We found that the PFL may play a dual role in the induction of oscillations. Under some conditions, the system can show bistability, and two Hopf bifurcation points confine an oscillation regime in the off state. For a strong stimulus above the threshold, transient oscillations last for a long period before the system switches to the on state. Quasistatic approximation was exploited to analyze this phenomenon. We proposed that the gradual transformation in the predomination of different feedback loops leads to the conversion from oscillation to bistability. The timescale of the PFL influences both the oscillation regime and the early-switching threshold for the stimulus. It is noteworthy that the above conclusions are applicable only to the example networks in Fig. 1. Our paper is organized as follows. The abstract model of combined positive and negative feedback loops is introduced in Sec. II. Interesting dynamic transitions of the system and an explanation for the underlying mechanisms are presented in Sec. III. A discussion and conclusion are presented in Sec. IV.

II. MODEL

All the gene regulatory networks in Fig. 1 include interlinked PFL and NFL. Their topology features are summarized in Table I. After some simplification, all the example networks comprise the NFL and PFL with similar architecture [except the PFL is somewhat different in Fig. 1(d)]. Furthermore, these networks share the same dynamic properties: the NFL alone is sufficient to produce oscillations, while the PFL can induce switchlike behaviors. Thus, it is plausible to elucidate the dynamics of these networks using an abstract model with the same topology.

The specific form of the model is largely derived from two models describing p53 dynamics where the interlinked p53-centered NFL and PFL can produce both oscillation and bistability [13,25], in agreement with desired dynamic properties. In the NFL, p53 induces *mdm2* mRNA to produce inactive Mdm2 protein, which can convert to the active form to promote p53 degradation; in the PFL, p53 transactivates *pten* expression to synthesize PTEN protein, which activates p53 by deactivating Mdm2 indirectly. If p53 is denoted by A, the three Mdm2-related forms by B_1, B_2, and B_3, and the two PTEN-related forms by C_1 and C_2, we obtained the abstract model as shown in Fig. 2. In the model, A transactivates B_1 and C_1, which are translated to B_2 and C_2. B_2 can convert to B_3, which promotes the degradation of A, enclosing a long NFL. On the other hand, C_2 promotes the conversion from B_3 to B_2, thereby enclosing a PFL. The level of A is regarded as the output of the system. The dynamics of the system are governed by the following ordinary differential equations [Eqs. (1)–(6)]:

$$\frac{d[A]}{dt} = k_{sa0} + k_{sa}\frac{S}{S + j_S} - k_{da}[B_3]\frac{[A]}{[A] + j_{da}} - k_{da0}[A], \tag{1}$$

$$\frac{d[B_1]}{dt} = k_{sb10} + k_{sb1}\frac{[A]^{n_1}}{[A]^{n_1} + j_{sb1}^{n_1}} - k_{db1}[B_1], \tag{2}$$

TABLE I. Common properties of the example networks in Fig. 1. (a)–(d) Simplification of the example IPNFLs into similar topology; (e) the abstract model. → and ⊣ represent activation and inhibition, respectively.

	PFL							NFL				
(a)	p53	→	PTEN	⊣	Mdm2	⊣	p53	p53	→	Mdm2	⊣	p53
(b)	HIF-1	→	miR-182	⊣	PHD2	⊣	HIF-1	HIF-1	→	PHD2	⊣	HIF-1
(c)	Notch1	→	RBP-Jκ	⊣	Hes1	⊣	Notch1	Notch1	→	Hes1	⊣	Notch1
(d)	Spo0A	→	KinA	→	Spo0A			Spo0A	→	Spo0E	⊣	Spo0A
(e)	A	→	C	⊣	B	⊣	A	A	→	B	⊣	A

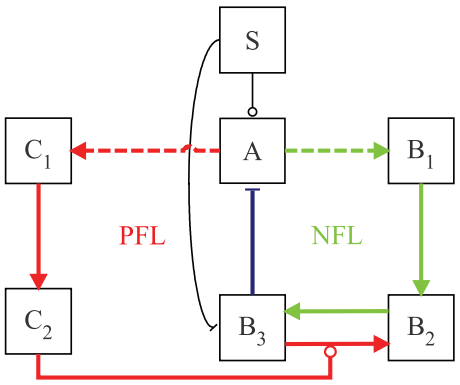

FIG. 2. Schematic diagram of the model of coupled positive and negative feedback loops. There are two main loops: the red (gray) one represents the positive feedback loop (PFL), the green (light gray) one represents the negative feedback loop (NFL), and the blue (dark gray) line represents their overlapping part. The induction of genes is represented by arrow-headed dashed lines. State transition of the proteins is denoted by arrow-headed solid lines. The activation and inhibition of the state transition are separately denoted by circle-headed and bar-headed solid lines.

$$\frac{d[B_2]}{dt} = k_{sb2}[B_1] - k_{acb2}\frac{[B_2]}{[B_2]+j_{acb2}} + k_{deb3}\frac{[C_2][B_3]}{[B_3]+j_{deb3}} - k_{db2}[B_2], \quad (3)$$

$$\frac{d[B_3]}{dt} = k_{acb2}\frac{[B_2]}{[B_2]+j_{acb2}} - k_{deb3}\frac{[C_2][B_3]}{[B_3]+j_{deb3}} - \left(k_{db30} + k_{db3}\frac{S}{S+j_S}\right)[B_3], \quad (4)$$

$$\frac{d[C_1]}{dt} = \tau\left(k_{sc10} + k_{sc1}\frac{[A]^{n_2}}{[A]^{n_2}+j_{sc1}^{n_2}} - k_{dc1}[C_1]\right), \quad (5)$$

$$\frac{d[C_2]}{dt} = \tau(k_{sc2}[C_1] - k_{dc2}[C_2]). \quad (6)$$

Here $[\cdot]$ represents the concentration of proteins or mRNAs. S is the strength of the stimulus, which promotes the production of A and degradation of B_3; their maximal rates are k_{sa} and k_{db3}, respectively. The transcriptional activation of B_1 and C_1 is described by Hill functions. The conversion between B_2 and B_3 is characterized by Michaelis-Menten kinetics since it is considered an enzymatic reaction. Each species, except B_3, degrades at a constant rate. Similar to the model by Brandman *et al.* [3], τ is considered as the timescale of C_1 and C_2 dynamics and is used to control the implicit time delay between the PFL and NFL. k_{sb1} and k_{sc1} are two key parameters modulating the strength of negative and positive feedback, respectively. The standard parameter settings are listed in Table II.

The units of parameters were determined such that the concentration of proteins is dimensionless. The above ordinary differential equations were numerically solved using Oscill8 (http://oscill8.sourceforge.net), and the bifurcation diagrams were also plotted using Oscill8. The time step of integration was 0.01. Unless otherwise specified, all initial values of the variables were their steady-state values at $S = 0$.

TABLE II. Standard parameter values in the model.

Parameter	Value	Parameter	Value	Parameter	Value
j_S	1	k_{sa0}	0.01	k_{sa}	0.3
k_{da0}	0.2	k_{da}	0.3	j_{da}	0.01
j_{sb1}	0.3	k_{sb10}	0.009	k_{db1}	0.1
n_1	4	k_{sb2}	0.2	k_{db2}	0.1
k_{acb2}	10	j_{acb2}	0.6	k_{deb3}	30
j_{deb3}	0.3	k_{db30}	0.1	k_{db3}	0.3
j_{sc1}	0.6	k_{sc10}	0.001	k_{dc1}	0.1
n_2	4	k_{sc2}	0.2	k_{dc2}	0.2

III. RESULTS

The system of IPNFLs can exhibit different dynamics such as bistability and oscillation, depending on the strength of feedback loops [9]. We will modulate the strength of feedback loops and the timescale of the PFL to investigate the system dynamics. We explore both the steady-state properties and transient dynamics during transitions from oscillation to the steady state. Moreover, we probe the potential link between the dynamics and biological function of IPNFL in some biological networks.

A. Dual role of the PFL in producing oscillations

It is known that an NFL is required but insufficient for oscillation [26]. Here the four-component NFL alone can produce persistent oscillations when its strength is strong enough [Fig. 3(a), top panel]. If the negative feedback is weaker, the system shows only damped oscillations and finally

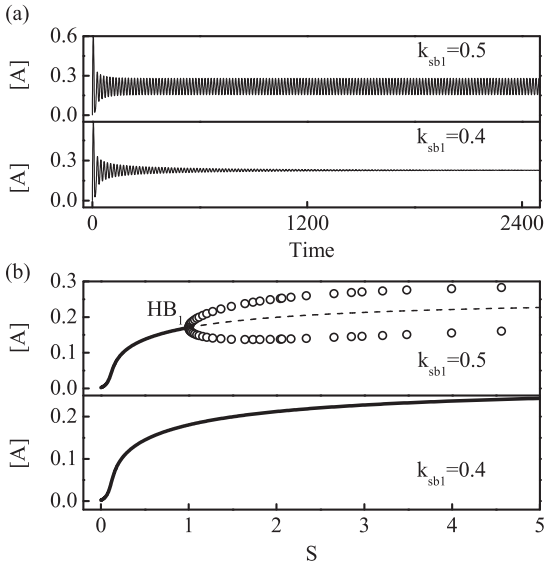

FIG. 3. Negative feedback is necessary but insufficient for oscillations. (a) Temporal evolution of $[A]$ in the single NFL at $S = 3$ with $k_{sc1} = 0$. $[A]$ exhibits persistent oscillations at $k_{sb1} = 0.5$ or damped oscillation before settling to a steady state at $k_{sb1} = 0.4$. (b) Bifurcation diagrams of $[A]$ versus S for $k_{sb1} = 0.5$ and 0.4. Solid and dashed lines denote stable and unstable steady states, respectively. Circles denote the maxima and minima of limit-cycle oscillations.

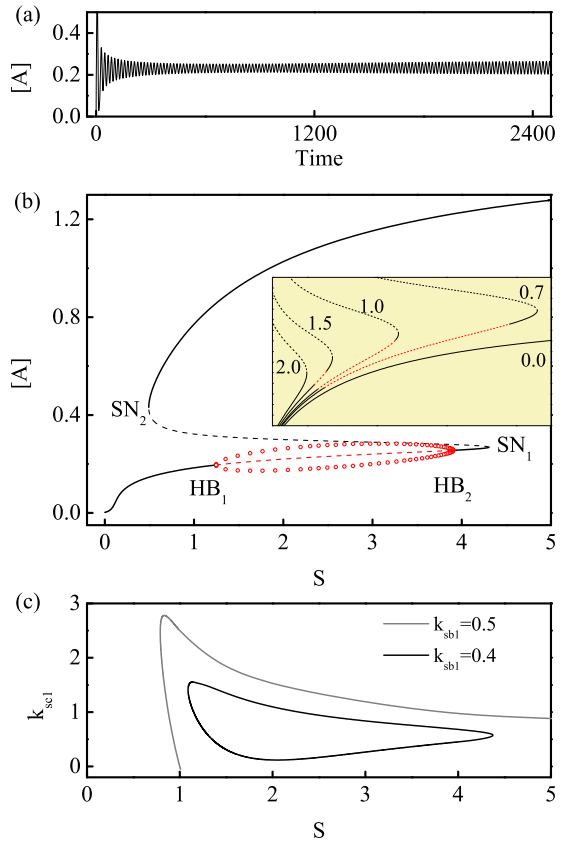

FIG. 4. Roles for positive feedback in oscillation. (a) Adding a PFL can tune the system into oscillation at $S = 3$ with $k_{sb1} = 0.4$ and $k_{sc1} = 0.5$. (b) Bifurcation diagram of $[A]$ versus S with $k_{sc1} = 0.7$, $k_{sb1} = 0.4$, and $\tau = 0.02$. The oscillation regime is marked by HB_1 and HB_2, and the red circles represent the minima and maxima of oscillations. The inset shows different diagrams for $k_{sc1} = 2.0$, 1.5, 1.0, 0.7, 0.0 (from left to right). The oscillation regimes for S are marked by red (gray) dashed lines. (c) Oscillation regimes in the S-k_{sc1} phase diagram with $k_{sb1} = 0.5$ (light gray) or 0.4 (black).

settles to a steady state for the same stimulus [Fig. 3(a), bottom panel]. Indeed, an oscillation region occurs in the bifurcation diagram of $[A]$ versus S with a stronger NFL [Fig. 3(b)]. Notably, a series of intermediates in the NFL contributes to the time delay required for oscillations [26]. A similar mechanism has been exploited in the core model of circadian rhythm including nuclear and cytoplasmic mRNAs and proteins [27].

We further investigated the role of PFL in producing oscillations under different conditions. When the negative feedback is too weak to induce oscillations, adding a PFL may result in persistent oscillations [Fig. 4(a)]. This result is consistent with the previous findings that the PFL may facilitate the induction of oscillation by providing additional time delay for the NFL [9,26].

The strength of the PFL is significantly modulated by the induced production rate of C_1, k_{sc1}. The bifurcation diagram of $[A]$ versus S depends heavily on k_{sc1}. When the NFL is weak and the PFL is strong enough, there exist two saddle-node bifurcations (SN_1 and SN_2) and two Hopf bifurcations (HB_1 and HB_2) on the lowest branch [Fig. 4(b)]. The thresholds of S at SN_1 and SN_2 are denoted by S_1 and S_2, respectively, while those at HB_1 and HB_2 are separately represented by H_1 and H_2 (hereinafter the same). Beginning with the off state at $S = 0$, the system shows low-amplitude oscillations for a moderate S or switches to the on state when S exceeds S_1. This feature was also reported in a modeling work on p53 dynamics [25]. The strength of positive feedback modulates the locations of HB_1 and HB_2 [Fig. 4(b), inset]. When k_{sc1} is very small, the system always stays in the off state; oscillations may occur over a wide range of intermediate k_{sc1} values. When k_{sc1} is large enough, the range of S for oscillation shortens to zero. Therefore, the PFL plays a dual role in modulating oscillations when the NFL alone is too weak to induce oscillations.

Furthermore, a two-parameter bifurcation diagram reveals the effects of the PFL on oscillation induction [Fig. 4(c)]. When the NFL is stronger, the range over S allowing for oscillation is rather wide for small k_{sc1}, but it shrinks quickly with increasing k_{sc1} (light gray curve). If negative feedback becomes weaker, the PFL with proper strength promotes oscillation, but the strong PFL suppresses oscillation (black curve). This dual role of the PFL can be understood as follows. Both the NFL and a proper time delay are required for oscillations. With the weak NFL, the PFL with proper strength facilitates oscillations by lengthening the time delay [26]. The very strong PFL cuts off the NFL by disrupting its negative arm, thereby repressing oscillations. Collectively, the role of PFL in inducing oscillation depends on the strength of feedback loops.

B. Spontaneous transition between dynamic modes due to alternation in the predomination of feedback loops

We have shown that the strength of positive feedback can modulate the range of S-admitting oscillation. When the PFL is very strong and is activated very slowly, no oscillation regime occurs in the bifurcation diagram [Fig. 5(a)]. Nevertheless, $[A]$ undergoes a series of oscillations before switching to the on state [Fig. 5(b)]. If S is slightly larger than S_1, $[A]$ oscillates for a long period and then switches to the on state [Fig. 5(b), top panel]. If S is much larger than S_1, the duration of oscillations is much shorter and the on state is reached more quickly [Fig. 5(b), bottom panel]. The transient pulses indeed appear in the dynamics of p53, HIF-1, Hes1, and Spo0A before a final decision-making for cellular outcome [12,17,21,24]. Our results show that transient behavior of the system cannot be revealed directly by bifurcation analysis. Other approaches are required to clarify the mechanism underlying the spontaneous transition between dynamic modes.

To this end, we focus on the dynamics around the off state in Fig. 5(b). Notably, the amplitude of oscillations varies dynamically [Fig. 6(a), the red upper and green lower lines]. The transient dynamics can be roughly divided into three stages: (1) early stage in which the amplitude drops gradually, (2) intermediate stage in which the amplitude slowly rises and then drops until the oscillation stops,and (3) late stage in which the concentration gradually climbs to the on state. Here we take a very small τ so that the kinetics become very slow and a quasistatic approximation can be applied to analyze the dynamics. Although such a small τ may be less meaningful for real biological networks, this quasistatic analysis should be effective to qualitatively explain the transient dynamics with

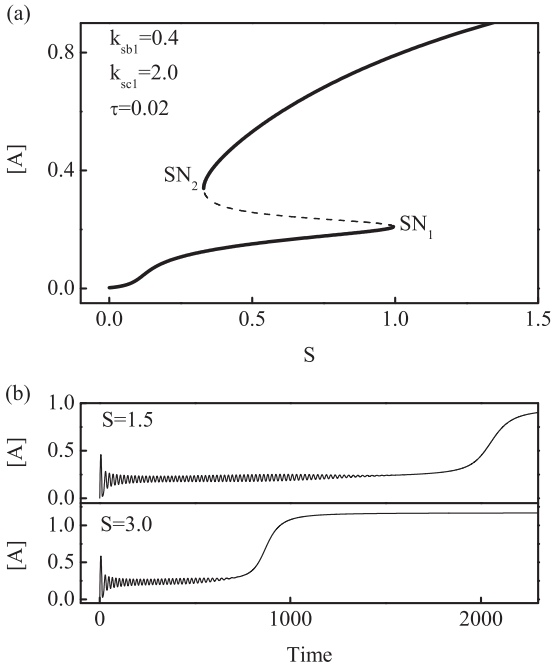

FIG. 5. Spontaneous transition between dynamic modes. (a) Bifurcation diagram of $[A]$ versus S with $k_{sb1} = 0.4$, $k_{sc1} = 2.0$, and $\tau = 0.02$. (b) Temporal evolution of $[A]$ for $S = 1.5$ and 3.0.

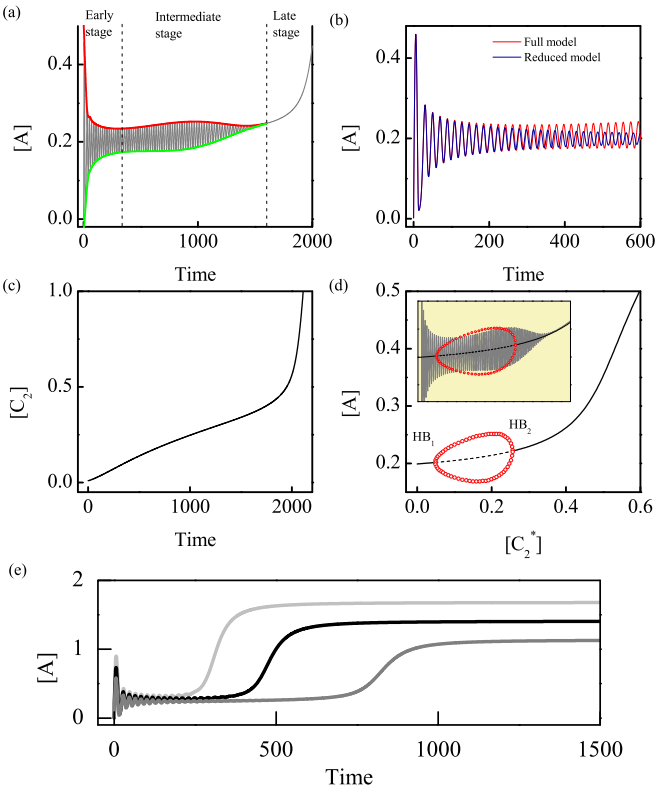

FIG. 6. Analysis on the transient dynamics. (a) Stages of the transient dynamics. The transient dynamics of $[A]$ in the upper panel of Fig. 5(b) can be roughly divided into three stages: early, intermediate, and late stage. (b) At the early stage, the dynamics of $[A]$ in the full model (red or light gray curve) are consistent with those in the reduced model with $[C_2^*] = 0.01$ (blue or dark gray curve). (c) Dynamics of $[C_2]$ with the same parameter setting as in (a). (d) Bifurcation diagram of $[A]$ versus $[C_2^*]$ in the reduced model. Red circles denote the maxima and minima of oscillations, which can be used to explain the variation in the amplitude of $[A]$ in the full model (the inset). (e) Transient dynamics vary with $k_{sa} = 0.24$, 0.30, 0.36 (from left to right). Here we set $k_{sb1} = 0.4$, $k_{sc1} = 2.0$ and $\tau = 0.02$, and all the other parameters are the same as those in Table I.

larger timescales. In this case, $[C_2]$ rises so slowly that in a short time interval, $[C_2]$ can be approximately considered a constant that regulates the dynamics of $[A]$. Thus, we built a reduced model by removing the equations of $[C_1]$ and $[C_2]$ [i.e., Eqs. (5)–(6)] and replacing $[C_2]$ in Eqs. (3)–(4) with a parameter $[C_2^*]$, which can be changed independently.

In the full model, the PFL is not activated at all at the early stage since $[C_2]$ is close to its basal level [Fig. 6(a)]. Indeed, when $[C_2^*]$ is set to the basal level, $[A]$ shows damping oscillations in the reduced model [Fig. 6(b), blue (dark gray) curve], coinciding perfectly with the early dynamics of $[A]$ in the full model [Fig. 6(b), red (light gray) curve]. This means that the NFL dominates at the early stage and induces damped oscillations, similar to the results in Fig. 3(a). At the intermediate stage, the PFL is enhanced gradually since $[C_2]$ rises almost linearly before reaching a higher level in the full model [Fig. 6(c)]. As shown in the bifurcation diagram of $[A]$ versus $[C_2^*]$ [Fig. 6(d)], the oscillation amplitude rises gradually and then drops quickly, because enhancing the positive feedback first promotes and then represses oscillation [Fig. 6(d), inset]. At the late stage, $[C_2]$ rises rapidly and thus $[A]$ switches to the on state [Figs. 6(c) and 6(d)]. Collectively, the multiphase dynamics of A reflect the dynamic competition between feedback loops: the NFL first predominates, and the PFL gradually strengthens until it prevails over the NFL. This result agrees well with the two-phase dynamics of p53 [13]. Together, if the NFL and PFL predominate sequentially in the early and late phases of system dynamics, a transition between distinct dynamics modes may appear.

To probe whether the multiphase dynamics hold true for different parameter values, we analyze the robustness of the transient dynamics. In this system, for example, fluctuating k_{sa} by 20% will influence the transient oscillation and the on state levels [Fig. 6(e)]. Moreover, the system can undergo at least two pulses and still switch to the on state with 20% changes in other parameters except n_1 and n_2. Therefore, the multiphase dynamics are robust to parameter variation and independent of parameter setting to a great extent.

C. Effects of the timescale of the PFL on oscillations and early switching

In general, the stimulus strength must exceed the upper threshold S_1 to turn on the switch if the system evolves from the off state [see Figs. 4 and 5]. Intriguingly, when the timescale of the positive feedback becomes rather large, the system switches to the on state even when S is much less than S_1. The resulting threshold, S^*, is called the early switching threshold [Fig. 7(a)]. Such an early switching was also reported in the model on p53 dynamics, and it may advance apoptosis induction by p53

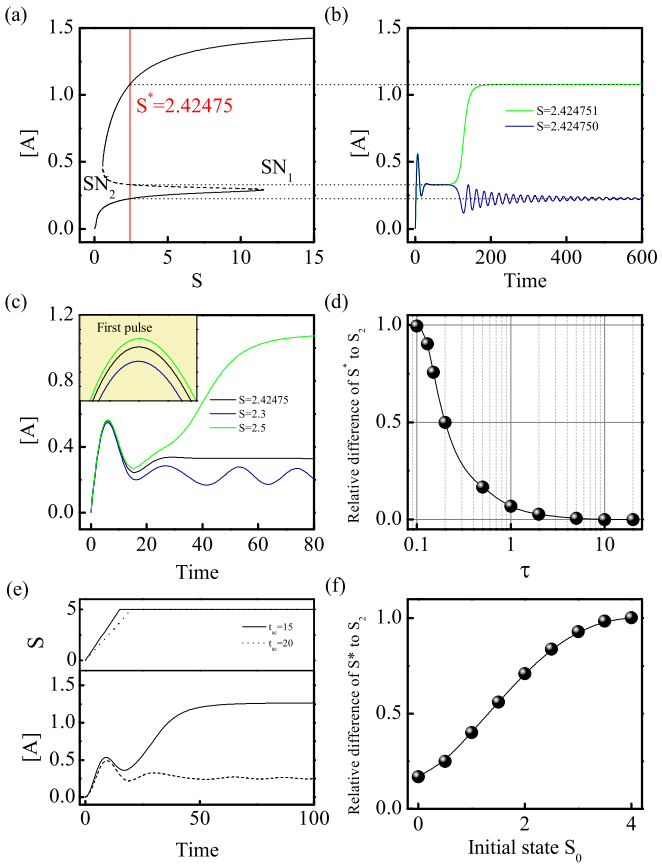

FIG. 7. Early switching to the on state. (a) Bifurcation diagram of $[A]$ versus S with $k_{sb1} = 0.4$, $k_{sc1} = 0.5$, and $\tau = 0.5$. The system switches to the on state when S is greater than $S^* \approx 2.42475$ (vertical dashed line). (b) Critical slowdown in the dynamics of $[A]$ with S slightly greater (light gray curve) or smaller (black curve) than S^*. (c) The time course of $[A]$ around the early switching threshold. The curve of $[A]$ dynamics at S^* can be considered as a critical curve (black curve). The inset is an enlarged view of the first pulse for different stimuli. (d) The curve of S^* position versus τ. The relative difference of S^* to S_2 is measured by $(S^* - S_2)/(S_1 - S_2)$, and the horizonal coordinate is logarithmic. (e) Time courses of S and $[A]$ for different increasing rate of S. The stimulus gradually rises at different rates to the same final value, S_{final}. Here $S_{\text{final}} = 5 < S_1$, and all parameters are the same as those in (a). (f) The curve of the relative difference of S^* to S_2 versus the initial stimulus strength S_0.

[25]. In the following, we will explore the potential mechanism behind early switching of the bistable system.

There exist three states for $[A]$ at S^*: a stable off state, unstable saddle, and stable on state [Fig. 7(a)]. Among them, the saddle is usually inaccessible in temporal evolution. In Fig. 7(b), $[A]$ exhibits critical slowdown when S is near S^*, like normal bistability around the saddle-node bifurcation point. Initially, there exists a transient high-amplitude pulse whose maximum remarkably exceeds $[A]$ at the saddle point. Then $[A]$ drops to its value around the saddle point and remains there for a long period. Finally $[A]$ converges to the on or off state depending on whether S exceeds S^*. Theoretically, the transient can last infinitely if $|S - S^*|$ is infinitely close to zero. For S close to S^*, there exists only subtle difference in the first pulse of $[A]$, while $[A]$ converges to distinct final states depending on S values [Fig. 7(c)]. Recent theoretical work has revealed that the potential landscape changes with the temporal variation in control parameters, and the separatrix of both basins of attraction in the bistable system moves dynamically [28]. Similarly, the switching to the on state will take place when the separatrix of two attractors is crossed. For fixed initial conditions, the fast kinetics in the PFL facilitate the phase trajectory to transverse the separatrix when S is larger than S^*. Therefore, quick activation of the PFL contributes to the early switching of the system.

We have shown that the system exhibits early switching to the on state when the timescale of the positive feedback is rather large. Obviously, changes in the timescale τ of C_1 and C_2 do not alter the steady states of the system. The curve of relative difference between S^* and S_2, $(S^* - S_2)/(S_1 - S_2)$, versus τ is plotted to show the effect of τ on the early switching of the system [Fig. 7(d)]. S^* drops monotonically with increasing τ. When τ is very small, S^* almost equals S_1, indicating that no early switching appears. The early switching threshold S^* moves left with increasing τ. When τ is large enough, S^* almost equals S_2. Together, the timescale of the positive feedback significantly modulates the threshold of stimuli for switching to the on state.

In the above cases, the stimulus strength always instantaneously jumps from 0 to S_{final}. It is necessary to assess whether the increasing rate of S affects the final state of the system. For simplicity, we assume that S increases linearly obeying the following equation:

$$\frac{dS}{dt} = \frac{S_{\text{final}}}{t_{ac}} H(S_{\text{final}} - S). \tag{7}$$

Here t_{ac} controls the increasing rate of S, and $H(S_{\text{final}} - S)$ is the Heaviside function. In Fig. 7(e), S increases at different rates to the same final value that is less than S_1. The system still switches to the on state in advance for $t_{ac} = 15$ (solid line), whereas the system converges to the off state for $t_{ac} = 20$ (dashed line). Thus, the increasing rate of S significantly influences the occurrence of early switching.

The stimulus strength at the initial state is denoted by S_0, which is fixed at 0 above. We found that S_0 affects the threshold of S for switching on the system [Fig. 7(f)]. With increasing S_0, S^* moves toward S_1. For S less than S_1, the system is more easily driven to the corresponding off state when S_0 gets closer to S_1. Taken together, the threshold for switching on the bistable switch is modulated by several factors including timescale of the kinetics, initial conditions, and the increasing rate of the stimuli.

Intriguingly, the value of τ also affects the position of Hopf bifurcation points in the diagram [Fig. 8(a)]. For smaller τ, the right Hopf bifurcation point HB_2 is located on the saddle-point branch (red triangle dot). The system can oscillate when S falls in the range between HB_1 and HB_2, and all the off states become unstable with $S > H_1$. For larger τ, HB_2 moves to the lowest branch (blue circle dot), and the actual oscillation regime narrows remarkably. Therefore, the timescale of the PFL affects the competition between the PFL and NFL. For rather large τ, fast kinetics of the PFL repress the NFL-induced oscillation.

For different τ, the system exhibits distinct behaviors in the off state. With a larger τ and a moderate S, $[A]$ may undergo

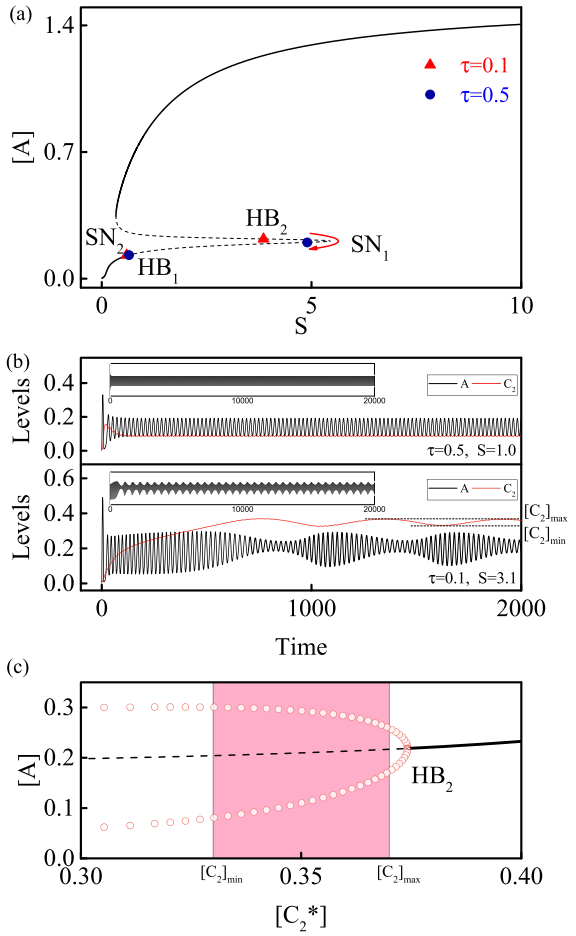

FIG. 8. Effects of timescale of the PFL on the system dynamics. (a) Bifurcation diagram of $[A]$ versus S with $k_{sb1} = 1.0$ and $k_{sc1} = 2.0$. The two pairs of Hopf bifurcation points correspond to the case of $\tau = 0.1$ (red triangles) and 0.5 (blue circles). (b) Dynamics of $[A]$ and $[C_2]$ with $\tau = 0.5$ and $S = 1.0$ (top panel), with $\tau = 0.1$ and $S = 3.1$ (bottom panel). The inset is the dynamics of $[A]$ for a long duration. (c) Bifurcation diagram of $[A]$ versus $[C_2^*]$ in the reduced model with $k_{sb1} = 1.0$ and $k_{sc1} = 2.0$.

uniform oscillations with almost fixed amplitude since $[C_2]$ almost drops to its basal level after transient rising and the oscillations are mainly induced by the NFL [Fig. 8(b), top panel]. With a smaller τ and a specific S, $[A]$ oscillates while the amplitude changes periodically [Fig. 8(b), bottom panel, gray curve]. This is analogous to amplitude modulation in radio broadcasting, and it is interesting to explore whether such dynamics exist in any biological systems. In the bifurcation diagram of $[A]$ versus $[C_2^*]$ for the reduced model, the amplitude of $[A]$ varies with $[C_2^*]$ [Fig. 8(c), pink (gray) area]. When $[C_2]$ is high enough, the PFL represses the oscillations of $[A]$ by disrupting the NFL. Then $[C_2]$ decreases due to the reduction in its transactivation rate. Therefore, $[C_2]$ exhibits a slow oscillation that modulates the fast oscillation of $[A]$.

IV. DISCUSSION

We developed an abstract model based on the p53 network model to illustrate the potential performance advantage of IPNFLs over single feedback loops. We found that the PFL plays a dual role in the regulation of oscillations. We paid more attention to transient dynamics during the transition between oscillation and bistability in some specific networks including the p53 network. With constant strong stimuli, the system can exhibit transient oscillations followed by gradual switching to the on state. The alternative predomination of feedback loops may govern the transition between the two dynamic modes. Moreover, early switching to the on state depends on the parameters and initial conditions when the positive feedback is activated quickly. It would be intriguing to validate early switching in biological networks. Taken together, our work may provide new insights into the performance advantages of IPNFLs over single feedback loops.

It is worthy to note that our conclusions are not applicable to all gene regulatory networks including IPNFLs, since transition between oscillation and bistability appears only in some particular networks. In other networks comprising IPNFLs, only oscillation or bistability alone may be observed. Underlying the cell cycle of Xenopus embryos, for example, combined NFL and PFL function only as a relaxation oscillator in which the NFL flips the PFL-induced bistable switch between on and off states repeatedly [6]. In the circadian rhythm systems, the PFL cooperates only with the NFL to produce oscillations [29]. Here our model mainly aims at the systems in which oscillation can be induced by the NFL, and the fully activated PFL can terminate the oscillations and push the system to high levels. All the examples in Fig. 1 can satisfy the above requirements to a great extent. Oscillation and bistability are two typical dynamic modes in gene regulatory networks, and it is interesting to identify more examples in which the system can transit between the two behaviors. Moreover, sufficient time delay in the NFL is required for oscillations [26]. In our model, the implicit time delay results from intermediate components in the NFL and hysteresis due to the PFL. Our results could be applicable to the case with explicit time delay in feedback.

In our model, the intensity of stimuli can regulate the level of the transcription factor and selective expression of its target genes, thereby modulating the competition between feedback loops. Our results may provide a plausible explanation for the bimodal and two-phase dynamics of p53 [11–13]. The NFL alone produces p53 oscillation for mild stimuli. The PFL is gradually activated to drive p53 level to the on state following transient oscillations for strong stimuli. The p53 level exhibits monotonic increasing due to direct activation of the PFL for extremely strong stimuli [13]. Moreover, the dynamic evolution in the domination of the NFL and PFL may contribute to the transition of dynamic modes in the Notch1-Hes1 system [18,19,30].

In conclusion, this work reveals that the system of IPNFLs may act as a flexible motif to produce multiple dynamic modes including oscillation and bistability under some specific conditions. It has been demonstrated that p53 dynamics control cell fates, so that alternation in the dynamic modes of p53 leads to different cellular outcome in response to DNA damage [11–13,31]. Our work suggests that IPNFLs may be exploited by cells to make a decision between different fates based on

different dynamic modes. We expect that our results on the transition between oscillation and bistability by modulating the stimulus strength could be validated and exploited in synthetic biology.

ACKNOWLEDGMENT

This work was supported by the National Natural Science Foundation of China (Grants No. 11574139, 31361163003, and 11175084).

[1] J. J. Tyson, K. C. Chen, and B. Novak, Curr. Opin. Cell Biol. **15**, 221 (2003).
[2] J. E. Ferrell Jr., Curr. Opin. Cell Biol. **14**, 140 (2002).
[3] O. Brandman, J. E. Ferrell Jr., R. Li, and T. Meyer, Science **310**, 496 (2005).
[4] X.-P. Zhang, Z. Cheng, F. Liu, and W. Wang, Phys. Rev. E **76**, 031924 (2007).
[5] P. Smolen, D. A. Baxter, and J. H. Byrne, Phys. Rev. E **79**, 031902 (2009).
[6] J. R. Pomerening, S. Y. Kim, and J. E. Ferrell Jr., Cell **122**, 565 (2005).
[7] T. Y.-C. Tsai, Y. S. Choi, W. Ma, J. R. Pomerening, C. Tang, and J. E. Ferrell Jr., Science **321**, 126 (2008).
[8] O. Brandman and T. Meyer, Science **322**, 390 (2008).
[9] X.-J. Tian, X.-P. Zhang, F. Liu, and W. Wang, Phys. Rev. E **80**, 011926 (2009).
[10] L. D. Mayo and D. B. Donner, Trends Biochem. Sci. **27**, 462 (2002).
[11] X. Chen, J. Chen, S. Gan, H. Guan, Y. Zhou, Q. Ouyang, and J. Shi, BMC Biol. **11**, 73 (2013).
[12] M. Wu, H. Ye, Z. Tang, C. Shao, G. Lu, B. Chen, Y. Yang, G. Wang, and H. Hao, Cell Death Dis. **8**, e3130 (2017).
[13] X.-P. Zhang, F. Liu, and W. Wang, Proc. Natl. Acad. Sci. USA **108**, 8990 (2011).
[14] G. D'Angelo, E. Duplan, N. Boyer, P. Vigne, and C. Frelin, J. Biol. Chem. **278**, 38183 (2003).
[15] T. J. Kelly, A. L. Souza, C. B. Clish, and P. Puigserver, Mol. Cell. Biol. **31**, 2696 (2011).
[16] Y. Li, D. Zhang, X. Wang, X. Yao, C. Ye, S. Zhang, H. Wang, C. Chang, H. Xia, Y.-c. Wang, *et al.*, Sci. Rep. **5**, 12495 (2015).
[17] J. Bagnall, J. Leedale, S. E. Taylor, D. G. Spiller, M. R. H. White, K. J. Sharkey, R. N. Bearon, and V. See, J. Biol. Chem. **289**, 5549 (2014).
[18] H. Hirata, S. Yoshiura, T. Ohtsuka, Y. Bessho, T. Harada, K. Yoshikawa, and R. Kageyama, Science **298**, 840 (2002).
[19] S. Agrawal, C. Archer, and D. V. Schaffer, PLoS Comput. Biol. **5**, e1000390 (2009).
[20] T. Kobayashi and R. Kageyama, Genes Cells **15**, 689 (2010).
[21] T. Kobayashi, H. Mizuno, I. Imayoshi, C. Furusawa, K. Shirahige, and R. Kageyama, Genes Dev. **23**, 1870 (2009).
[22] K. L. Ohlsen, J. K. Grimsley, and J. A. Hoch, Proc. Natl. Acad. Sci. USA **91**, 1756 (1994).
[23] S. H. Shafikhani and T. Leighton, Curr. Microbiol. **48**, 262 (2004).
[24] J. H. Levine, M. E. Fontes, J. Dworkin, and M. B. Elowitz, PLoS Biol. **10**, e1001252 (2012).
[25] K. B. Wee, U. Surana, and B. D. Aguda, PLoS ONE **4**, e4407 (2009).
[26] B. Novak and J. J. Tyson, Nat. Rev. Mol. Cell Biol. **9**, 981 (2008).
[27] D. Gonze, J. Halloy, and A. Goldbeter, Proc. Natl. Acad. Sci. USA **99**, 673 (2002).
[28] B. Verd, A. Crombach, and J. Jaeger, BMC Syst. Biol. **8**, 43 (2014).
[29] K. Lee, J. J. Loros, and J. C. Dunlap, Science **289**, 107 (2000).
[30] H. Shimojo, T. Ohtsuka, and R. Kageyama, Neuron **58**, 52 (2008).
[31] J. E. Purvis, K. W. Karhohs, C. Mock, E. Batchelor, A. Loewer, and G. Lahav, Science **336**, 1440 (2012).

Correction: The originally published Figs. 4 and 8 contained errors and have been replaced.